

A preliminary threshold model of parasitism in the Cockle *Cerastoderma edule* using delayed exchange of stability

E A O'Grady¹, S C Culloty², T C Kelly², M J A O'Callaghan¹,
D Rachinskiy^{1,3}

¹ Department of Applied Mathematics, University College Cork, Ireland

² School of Biology, Earth and Environmental Sciences, University College Cork, Ireland

³ Department of Mathematical Sciences, The University of Texas at Dallas, Richardson, USA

E-mail: dmitry.rachinskiy@utdallas.edu

Abstract. Thresholds occur, and play an important role, in the dynamics of many biological communities. In this paper, we model a persistence type threshold which has been shown experimentally to exist in hyperparasitised flukes in the cockle, a shellfish. Our model consists of a periodically driven slow-fast host-parasite system of equations for a slow flukes population (host) and a fast *Unikaryon* hyperparasite population (parasite). The model exhibits two branches of the critical curve crossing in a transcritical bifurcation scenario. We discuss two thresholds due to immediate and delayed exchange of stability effects; and we derive algebraic relationships for parameters of the periodic solution in the limit of the infinite ratio of the time scales. Flukes, which are the host species in our model, parasitise cockles and in turn are hyperparasitised by the microsporidian *Unikaryon legeri*; the life cycle of flukes includes several life stages and a number of different hosts. That is, the flukes-hyperparasite system in a cockle is, naturally, part of a larger estuarine ecosystem of interacting species involving parasites, shellfish and birds which prey on shellfish. A population dynamics model which accounts for one system of such multi-species interactions and includes the fluke-hyperparasite model in a cockle as a subsystem is presented. We provide evidence that the threshold effect we observed in the flukes-hyperparasite subsystem remains apparent in the multi-species system. Assuming that flukes damage cockles, and taking into account that the hyperparasite is detrimental to flukes, it is natural to suggest that the hyperparasitism may support the abundance of cockles and, thereby, the persistence of the estuarine ecosystem, including shellfish and birds. We confirm the possibility of the existence of this scenario in our model, at least partially, by removing the hyperparasite and demonstrating that this may result in a substantial drop in cockle numbers. The result indicates a possible significant role for the microparasite in this estuarine ecosystem.

1. Introduction

Parasites are now widely recognised to play an important role in the structuring and functioning of ecological communities. In the estuarine systems of the south western USA, for example, Kuris *et al.* (2008) showed that parasite biomass “exceeded that of top predators” while the biomass of trematodes “equalled” that of the most abundant birds, fish and crustacea. Macroparasites, such as digenetic trematodes (also commonly known as flukes), have complex life cycles with several intermediate hosts and complex transmission dynamics to their final, usually vertebrate, hosts. Although it has been known for some time that the flukes themselves may

be parasitized by microparasites, the general importance of this relationship in the population dynamics of the interacting species has only recently been recognised (Raffel *et al.* 2008). The dynamics of many host-parasite relationships are subject to thresholds of several different types (Getz and Pickering, 1983; Heesterbeek and Roberts, 1995; Deredec and Courchamp, 2003; Kalachev *et al.*, 2011). In this section, we model the impact of a “persistence” type threshold in a hyperparasitised fluke which infects a common estuarine bivalve mollusc – the cockle *Cerastoderma edule*. A persistence-type threshold is relevant to parasites and is characterised by a necessary number or density of hosts for parasite maintenance (*sensu* Deredec and Courchamp, 2003). We begin by describing in more detail the main species involved in the study.

1.1. The Cockle

The cockle *Cerastoderma edule* populates estuarine regions from the Barents Sea to Morocco, including the coastlines of Britain and Ireland, the area in which this study was undertaken. Not only is this species of commercial importance, but it also plays a significant role in estuarine ecosystems as an important food source for birds, fish and crustaceans as well as in the dynamics and stability of the sediment. Cockle densities at different sites can be highly variable with 1000 per square metre not unusual but as many as 54,400 being recorded (Ducrotoy *et al.*, 1991). A range of variables control cockle population dynamics, including biotic influences such as bioturbation (that is burrowing activity and aeration of sediment), predation, parasitism and food availability together with abiotic factors such as temperature, immersion time, water velocity and sediment dynamics (Gam *et al.*, 2010). In particular, recruitment is significantly affected by predation by species such as the shrimp *Crangon crangon* (see for example, Beukema and Dekker, 2005).

1.2. The Macroparasite - the fluke

In intertidal ecosystems, flukes are the dominant parasite group (Mouritsen and Poulin, 2002). These macroparasites exert two influences; firstly as part of the living diversity, and secondly as diversity indicators, because their presence is linked to the richness of the free living fauna (their hosts) as demonstrated by Hechinger *et al.* (2007), thereby acting as a proxy for ecosystem health, (Hudson *et al.* 2006). These digenetic trematodes generally have three hosts in their life-cycle: a definitive host where the parasite reaches sexual maturity, a molluscan first intermediate host in which asexual reproduction occurs, and a second intermediate host which provides the vehicle for transfer back to the definitive host (Esch *et al.*, 2002).

Cockles are first or second intermediate hosts of, at least, 16 fluke species with complex life cycles involving 2-3 hosts (de Montaudouin *et al.*, 2009; Russell-Pinto *et al.*, 2006). This diversity in parasite infracommunities seems to be possible due to the observed high degree of spatial segregation of parasite species within their cockle host (Rohde, 1994). One such fluke is *Meiogymnophallus minutus*, which is one of four sibling species, all of which infect cockles of the genus *Cerastoderma*. The fluke can be found in the mantle epithelium of the cockle (Bowers *et al.*, 1996; de Montaudouin *et al.*, 2009). The fluke has a body length of 240-350 μm and a width of about 150 μm (Russell-Pinto, 1990). This trematode is a member of the Family Gymnophallidae, with the bivalve mollusc *Scrobicularia plana* being the first intermediate host, *C.edule* the second intermediate host, and the oystercatcher *Haematopus ostralegus* - a widely distributed shorebird - the final, or definitive, host. This cycle is described schematically in Figure 1.

It has been demonstrated that larval stages of *M. minutus* released from the first intermediate host and dispersed via water currents, passively locate their second intermediate host within a distance of a few hundred metres, where they encyst becoming metacercariae. These do not reproduce and therefore population growth within the cockle is solely due to the incremental effects of immigration. The impact of *M. minutus*, when present in large numbers, is to inhibit

the tight closing of the shell valves. Consequently, these cockles are often found, shell gaping upwards, close to the surface of the sand (Bowers *et al.*, 1996). Cockles infected with flukes suffer from a range of different effects such as impaired burrowing, reduced growth, increased mortality and reduced tolerance to opportunistic microparasitic infections (Lauckner *et al.*, 1983; Wegeberg and Jensen, 1999; 2003).

In a study conducted along the Northeast Atlantic, this fluke was found to be the most abundant and widespread trematode in cockles (de Montaudouin *et al.*, 2009) from the Wadden Sea in the north to Morocco in the south (Gam *et al.*, 2008). This distributional range is linked to large scale migrations of shorebirds (Thieltges and Reise, 2006). In previous studies the prevalence of *M. minutus* had been found to range from up to 48% in the Wadden Sea, (Thieltges and Reise, 2006), to as much as 100% in Arcachon Bay, France, (de Montaudouin *et al.*, 2000), in Merja Zerga in Morocco (Gam *et al.*, 2008) and at a number of sites along the south coast of Ireland (Fermer *et al.*, 2011).

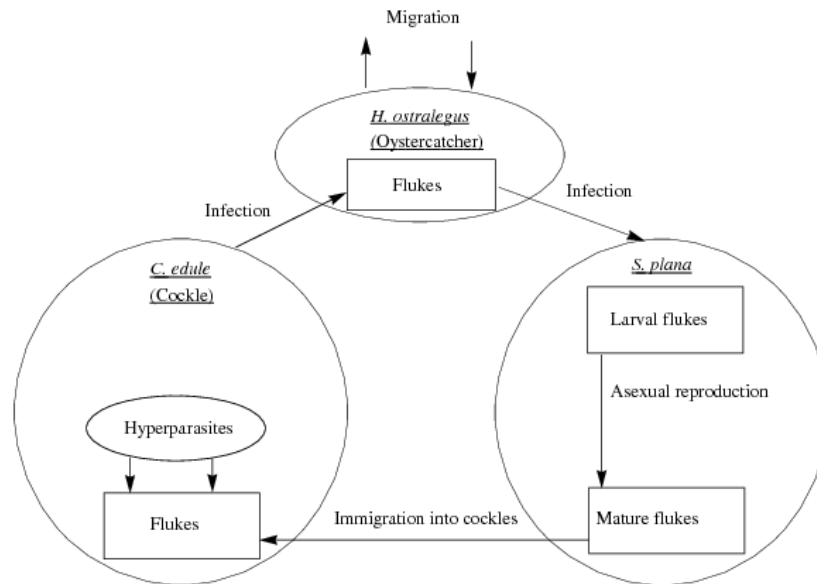


Figure 1. Flow chart showing the interactions of species involved and the life-cycle of the fluke *M. minutus*.

1.3. The Hyperparasite

Microsporidia are obligate intracellular eukaryotic microparasites, ranging in size from about 3 to 6 μm , most closely related to the Fungi (Troemel *et al.*, 2008). It is clear that they are up to two orders of magnitude smaller than the fluke. They infect both vertebrates and invertebrates and include a number of species that are found in humans (Didier *et al.*, 2004). Johnson *et al.* (2010) describe eight microsporidians, including *Unikaryon legeri* – the subject of this study, that are hyperparasites of various digenean trematodes which they classify as predators of the flukes. Although not germane to this study, the issue of whether *U. legeri* is a parasite (i.e. hyperparasite) or a predator needs to be addressed by future research because of the implications for the population dynamics of the interacting species.

1.4. Interaction between *M. minutus* and *U. legeri*

Spatial variation in the presence of the hyperparasite, *U. legeri*, was found by Fermer *et al.* (2010) when cockles ($N = 50$ at each site) were screened at 14 separate locations on the south coast of Ireland in July 2007. Hyperparasitism occurred at 8 out of the 14 sites and was prevalent only in cockles heavily infected with the fluke. Of particular significance was the fact that *U. legeri* was not present where the burden of *M. minutus* was less than approximately 185 metacercariae per cockle (Fermer, 2009). This low burden of metacercarial flukes within the cockle appears to be a threshold enabling infection with the hyperparasite. It is clearly evident therefore, that the threshold is that of a persistence type as defined above. It will ultimately determine the duration of infection, as seasonal effects will impact strongly on the average numbers of flukes in the cockles due to their temporal life-cycle.

It has been shown that hyperparasitism results in the death of a high proportion of the infected flukes. Due to hyperparasite-induced mortality, the entire metacercarial population has to rebuild every year. Hyperparasitism is thus a very important factor controlling fluke infrapopulation size and the overall dynamics of *M. minutus*.

1.5. Structure of the paper

In the next section we present and discuss a model of the hyperparasitised flukes in a cockle. This model is then incorporated as a subsystem in a larger ecosystem model, which is formulated and tested in Section 3. The multiscale analysis technique we use is close the method described by Nizette *et al.* (2006). The last section contains conclusions.

2. Fluke-Hyperparasite model

We present a mathematical model which describes the subsystem occurring in the individual cockle. In particular, we model the threshold population of flukes inside a cockle that is needed to provide a sufficient environment for the parasite population to grow and persist. As explained above, when fluke populations are less than 185 per cockle (Fermer, 2009), there are no hyperparasites present. On exceeding this threshold number of flukes, there is a significant change in the dynamics of both populations whereby the hyperparasite population grows, attacks and can kill part of the fluke population. The parasite has a regulatory effect on the fluke population which appears to be unique (see Raffel *et al.*, 2008).

2.1. Threshold model development

Flukes enter the cockle through immigration as outlined above. We assume a natural death rate of flukes and an interaction between the flukes and the hyperparasites that we consider to be of a parasitic type. On the basis of these assumptions, we write the following equation for the rate of change of the fluke population:

$$\text{Rate of change of fluke population} = (\text{Immigration term}) - (\text{Natural death rate}) - (\text{Death due to hyperparasites}),$$

which leads to the equation:

$$\frac{dF}{dt} = a(t) - \delta F - \lambda H,$$

where F is the fluke population, H is the hyperparasite population, the derivative dF/dt represents the rate of change of fluke population and $a(t)$ represents a time-dependent immigration rate. The term $-\lambda H$ represents the death rate of flukes due to the hyperparasites. As a parasitic type term, we assume that the damage caused by the hyperparasite to a single fluke is proportional to the mean number that the fluke carries, that is, H/F . Thus the decrease in the overall fluke population will be proportional to H . Here λ is a positive constant representing the number of flukes lost per hyperparasite per unit time.

For the hyperparasite population, we assume a natural death rate in the absence of flukes, a positive growth term due to the exploitation of their hosts, and a compensating term to reflect the damage that host mortalities have on the population:

$$\text{Rate of Change of parasite population} = - (\text{Death rate}) + (\text{Growth term due to parasitism on flukes}) - (\text{Compensating term}).$$

The second, growth, term here was developed as follows. The rate of production of hyperparasite transmission stages is proportional to H . The magnitude of the proportion of these hyperparasites that are successful in infecting flukes is characterised by a term reflecting the relative density of hosts, $F/(F_0 + F)$, where F_0 is a measure of the transmission efficiency, and F is the fluke population, as described in general terms in Anderson and May (1978). A large F_0 indicates that this efficiency is low and is the one that we use. Under this assumption, that only a small proportion of the hyperparasite transmission stages actively infect flukes, the growth term in the hyperparasite population is proportional to HF .

The compensating term reflects the fact that as it kills its host, a certain proportion of hyperparasites are also lost. An important factor needing consideration here is the distribution of hyperparasites in the flukes. Consequently, we note that as hyperparasites damage the fluke population at a rate proportional to H , they themselves will suffer loss proportional to H multiplied by a proportion of the average distribution H/F . We introduce a constant of proportionality f , to indicate this distribution proportion of hyperparasites on flukes. We will describe this coefficient in greater detail below. The equation for the rate of change of hyperparasites can then be written as:

$$\frac{dH}{dt} = -cH + dHF - \frac{f\lambda H^2}{F}.$$

It is common for systems to have dynamics that interact on differing timescales (see for example, Etchehoury and Muravchik; 2003) as described already, and so we now introduce one important assumption to this last equation. We will require that the interval over which the hyperparasite population replicates and undergoes transmission occurs on a timescale much shorter than the corresponding interval of the fluke population. This is reasonable given the fact that the hyperparasites are several orders of magnitude smaller than the flukes as mentioned above. To account for this mathematically, we introduce a new parameter ε in Eq. (2.1) and assume $0 < \varepsilon \ll 1$. Therefore we obtain the equations:

$$\frac{dF}{dt} = a(t) - \delta F - \lambda H, \tag{1}$$

$$\varepsilon \frac{dH}{dt} = -cH + dHF - \frac{f\lambda H^2}{F}. \tag{2}$$

The last term in Eq. (2) can be used to model the occurrence of over-dispersion of hyperparasites on flukes. Over-dispersion means that the majority of flukes carry few numbers of hyperparasites, while a minority are greatly infected. Thus, the death of a fluke results in a greater than average proportion of hyperparasites being lost. In this last term, we are concerned with those hyperparasites living on, and killing flukes, and we reason that the interaction occurs on timescales of that of the fluke. Thus, when we wish to examine cases of over-dispersion, it is meaningful to examine the value of the combination, $f\lambda/\varepsilon$. In particular, values of this ratio greater than one indicate over-dispersion.

Comparing our model with that described by Anderson and May (1978), it can be seen that the equation for our host, the fluke, equation is similar except that we have an immigration term that has a seasonal dependence instead of a natural birth rate, making the dynamics different. In the hyperparasite equation, we have an identical death rate and our birth rate

Table 1. Parameter values and units used in the model.

Parameter	Description	Value
a	Fluke immigration	20
δ	Fluke natural death rate	1/25
λ	Fluke death due to hyperparasitism	1/800
ε	Timescale separation parameter	1/5000
c	Hyperparasite natural death rate	185 d
d	Growth rate of Hyperparasite	1/3500

term is comparable in the regime where only a small fraction of the hyperparasite population is successful in infecting the flukes as discussed above. The compensating term is equivalent to Anderson and May's term for host-death induced parasite mortality, although written here in a different manner. We also have the notable difference of the differing time scales as introduced through the small parameter ε . This will be shown to have a major impact on the dynamics of the system.

Table 1 shows typical parameter values used in the model. Although direct experimental measurement of parameters is difficult, we can reason that there is a basis for the order of magnitude of the values used here. We use a reasonable monthly immigration rate of 20 here, particularly to examine the interesting behaviour of the threshold phenomenon. Natural death rates of both flukes and hyperparasites, δ and c respectively, are usually much less than 1, and we require that $c > \delta$ due to the fact that host deaths result in large numbers of parasite deaths. The parameter d is taken to be small here, to prevent too large a population of hyperparasites. The fluke death rate due to hyperparasitism, λ , is chosen here so that the hyperparasites have an impact on fluke population and regulate their growth. In the case of over-dispersion of hyperparasites, we want $f\lambda/\varepsilon$ greater than one and for our simulations we take a value of 5. We will see in the next section that the ratio c/d marks a point where the hyperparasite population goes to zero, or to a non-zero population, giving immediately the value used for c , if we take this to be the threshold population and assume it to be 185 (shown below).

2.2. Preliminary discussion

Two equilibria are possible in the system of Eqs. (1) and (2) with constant immigration term $a(t) \equiv a$, namely zero- and non-zero hyperparasite population equilibria, dependent on the parameters and the threshold effect we wish to model. Taking, a , the constant rate of immigration of flukes into the cockle, as a bifurcation parameter, a transcritical bifurcation can be shown to occur at $a = c\delta/d$. This transcritical bifurcation is evident as shown by Figure 2. A transcritical bifurcation indicates that a stable positive solution branches from the zero hyperparasite solution at the bifurcation point. In the current case, the zero hyperparasite equilibrium becomes unstable after the transcritical bifurcation while the positive, non-zero, hyperparasite population becomes stable. Thus, solutions after the transcritical bifurcation are attracted to the non-zero trajectory, while solutions before the transcritical bifurcation tend to the stable zero hyperparasite equilibrium. Therefore, the zero-hyperparasite equilibrium is stable if the condition $a/\delta < c/d$ is satisfied. The positive equilibrium exists and is stable if the opposite inequality holds. This figure is the same for all values of the time scale separation parameter ε . We see by Table 1, that both sides of the inequality have units of flukes. Thus we recognise that the number of flukes determines the stabilities of the zero and non-zero hyperparasite populations, and thereby, the dynamics of the system. In a real-life system, the immigration

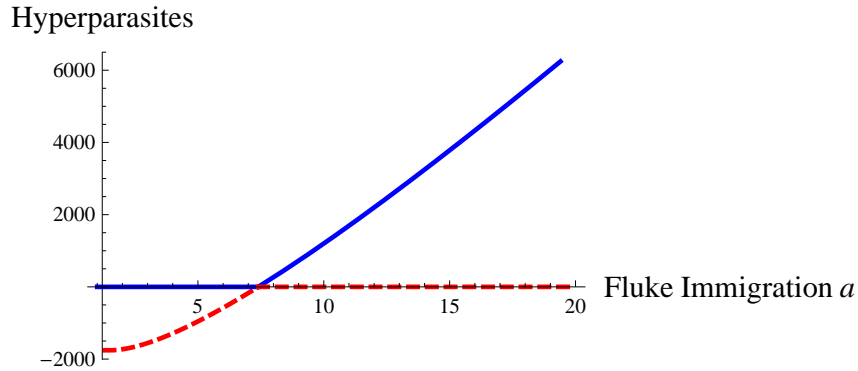


Figure 2. Bifurcation diagram showing fluke immigration rate parameter a on the horizontal axis with hyperparasite population on the vertical axis. Transcritical bifurcation point evident at $a = 7.4$, where for this parameter set $(a/\delta) = (c/d)$. Here, the previously stable zero hyperparasite solution exchanges stability with the previously unstable non-zero solution. It is evident that for this parameter set, hyperparasites are absent for a less than 7.4 and present above this value. Blue solid lines indicate stable solutions, red-dashed lines indicate unstable solutions. Here, the parameter values, apart from the bifurcation parameter a , are given in Table 1.

term varies temporally due to migratory patterns of birds who consume the cockles infected with parasites, which ultimately control the cycle of fluke reproduction, and also due to temperature variation and perhaps other abiotic influences. If $a(t)$ changes abruptly between two values, we obtain a switching system forced by a square wave function. Such a type of function to model the temporal influx of a species has been used previously in, for example, Holt *et al.* (2003). For example, at certain times of the year, the system can be attracted towards the zero-hyperparasite equilibrium due to no fluke immigration and for the rest of the year towards the positive equilibrium, shown in Figure 3.

2.3. Singular perturbation and stability exchange

First we examine the condition for the bifurcation point evident in system (1), (2).

Taking this system with constant immigration a , we wish to examine the stability of the equilibrium $(F^*, H^*) = (a/\delta, 0)$. The jacobian matrix of this system is

$$\begin{pmatrix} -\delta & -\lambda \\ 0 & (-c + dF)/\varepsilon \end{pmatrix}.$$

Hence, the eigenvalues are

$$\mu_1 = -\delta, \quad \mu_2 = (-c + dF)/\varepsilon.$$

For stability of the equilibrium $(F^*, H^*) = (a/\delta, 0)$, we require $\mu_1, \mu_2 < 0$ (both eigenvalues are real in this case). Since μ_1 is negative by definition ($\delta > 0$), the equilibrium is stable for $c > dF^* = da/\delta$, with the transcritical bifurcation occurring at

$$\frac{a}{\delta} = \frac{c}{d}.$$

For $\varepsilon \ll 1$, Eqs. (1) and (2) become a singularly perturbed system with the hyperparasite being the fast variable (see above and, for example, Veliov, 1997). Systems of this kind, where the small parameter ε tends to zero, lend themselves to analysis of a reduced initial value problem,

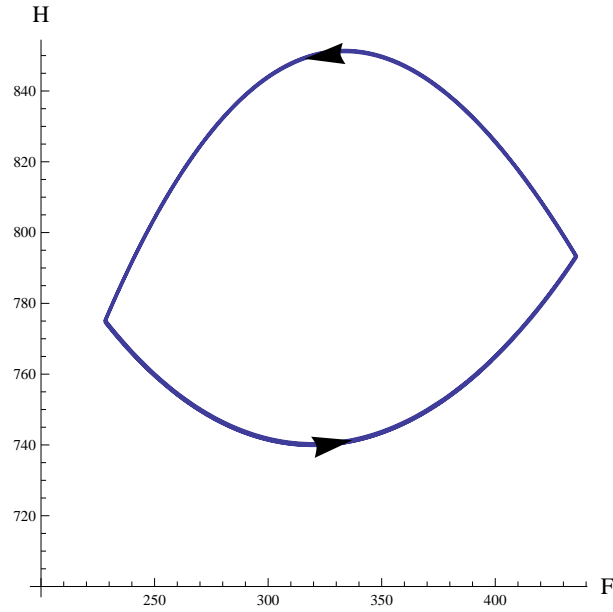


Figure 3. We include for illustrative purposes the stable periodic regime of system (1), (2) with the fluke immigration rate a switching periodically between the values $a = 0$ and $a = 70$. Here $\varepsilon = 1$, i.e. both populations evolve on the same timescale, $c = 185d$, $f = 0.9$, $\delta = 1/25$, $d = 0.00031$ and $\lambda = 1/50$. It can be seen that when immigration switches on, there is attraction towards the non-zero equilibrium, at least after the threshold number of flukes is reached. When immigration ceases, the system turns back and evolves towards the zero equilibrium, now stable at this time.

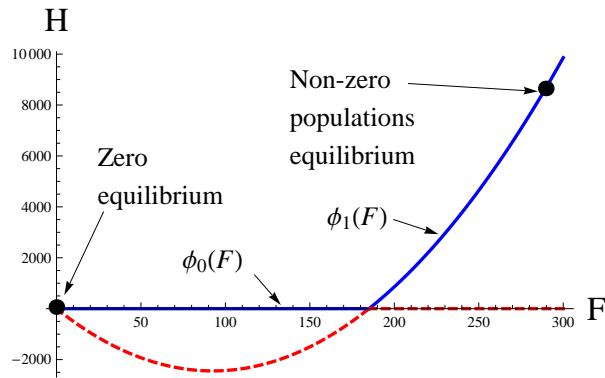


Figure 4. Intersecting critical curves $H = \phi_0(F)$, $H = \phi_1(F)$ of system (1) and (2) with parameter values shown in Table 1. Solutions of the dynamical system evolve on these curves, depending on stability of the equilibria. Two equilibria for the populations are indicated, and these depend on the value of a . When $a = 20$, immigration is switched on and solutions tend to the non-zero equilibrium. In this case, the zero equilibrium becomes unstable. When immigration is switched off, $a = 0$, the system tends towards the stable zero equilibrium.

which is one-dimensional in this case. Indeed, the trajectories of the singularly perturbed system spend most of the time near the critical manifold, actually a curve in this case, which is defined by setting the right hand side of the fast hyperparasite equation to zero, yielding the two roots

$$H = \phi_0(F) \equiv 0, \quad H = \phi_1(F) = F(dF - c)/(f\lambda),$$

(see Figure 4). The critical curve, which we mention here, indicates a curve that is quickly approached by solutions which then follow this curve on the $H - F$ plane. The curve given by $H = \phi_1(F)$ is a parabola. The threshold we model is the intersection of the two branches of the critical curve, that is the point $F = c/d$, because the hyperparasite population is always near zero below this point and is positive, at least sometimes, above it. Thus, we realise that this results in either positive numbers of hyperparasites, or zero hyperparasites, depending on the fluke population and the value of c/d , which we take now to be equal to 185. The picture shown in Figure 4, can be interpreted either as the phase plane of Eqs. (1) and (2), or as the bifurcation diagram of the fast equation (2), in which the slow variable F is treated as a parameter. Stable and unstable equilibrium points of Eq. (2) are shown by the solid and dashed lines respectively, with the transcritical bifurcation at the intersection point where $F = F_C = c/d$, which is the threshold value ($F_C = 185$).

While a trajectory closely follows one of the curves $H = \phi_k(F)$, the dynamics of the slowly varying fluke population is approximated by the reduced equation

$$\frac{dF}{dt} = a(t) - \delta F - \lambda \phi_k(F). \quad (3)$$

In the vicinity of the critical curve, solutions evolve on timescale equivalent to that of the fluke population, that is slow relative to the hyperparasite population. In our interpretation, the hyperparasite population is detectable when a trajectory is close to the positive branch $H = \phi_1(F)$ of the critical curve, and becomes undetectable when the trajectory switches to the zero branch $H = \phi_0(F) \equiv 0$. The scenario where a trajectory switches from one branch to the other at their intersection point $(F, H) = (F_C, 0)$ is known as an immediate exchange of stabilities, see the descending part of the trajectory in the left panel of Figure 5. It is evident from this figure that a different behaviour also arises where the trajectory stays in the neighbourhood of the unstable zero branch for a certain time after passing the point $F = F_C, H = 0$. The trajectory then follows a fast sharp transition from approximately a point $F = F_{th}, H = 0$, with $F_{th} > F_C$, to the stable branch $H = \phi_1(F)$, that is the scenario known as a delayed exchange of stability (see the ascending part of the trajectory in the left panel of Figure 5). It is clear therefore, that our system exhibits both *immediate* and *delayed* stability exchange, namely as the populations decrease and increase respectively. The immediate exchange of stability at F_C is defined by the parameters of the system, while the point of delayed stability exchange at F_{th} is defined by the dynamics of the system and varies for different trajectories. In particular, it is dependent on how long the value of $a(t)$ is equal to zero and the minimum value reached by the fluke population, F_{min} .

2.4. Seasonally forced model

We see that, in accordance with the different biologies of the interacting species, the faster timescale of the hyperparasite life cycle results in two thresholds as shown in the left panel of Figure 5. Nevertheless, the transcritical bifurcation point amply illustrates the overall threshold behaviour of the system.

In the above section we developed a model to describe the hyperparasite-fluke interaction within a cockle and the presence of a persistence-type threshold. We now address seasonal effects. Seasonality plays an important role within the system, as effects such as temperature,

bird migration, pollution, and other possible abiotic and biotic factors as mentioned earlier, will all lead to variations in the populations under consideration.

As a first approach, we consider Eqs. (1), (2) with a square wave, or switch-type immigration term. This means that the fluke immigration is a positive constant for part of the year, and zero for the rest. This is a realistic model for our system as flukes mature within *S. plana*, and are actively moving and swimming after having been artificially released, only at particular intervals of the year. In particular, Fermer *et al.* (2010) found that these stage cercariae appeared from June through October, and were the dominant developmental stage from July to October. The square wave switching model is also easier to analyse mathematically than other periodic patterns of immigration including the sinusoidal type, to be mentioned later.

We introduce the square wave immigration term $a(t) \equiv a(t+T)$ in Eq. (1) where $a(t) = A > 0$ for part of the year and zero otherwise, such as

$$a(t) = \begin{cases} A, & 0 \leq t \pmod{T} \leq \tau \\ 0, & \tau < t \pmod{T} < T = 12 \end{cases} \quad (4)$$

where there is immigration over τ months, and the population suffers from natural death and hyperparasitism as before. As an initial approximation, we take the value of τ to be 5, meaning we allow immigration for five months in the year, in keeping with experimental findings described above. A number of important population points and times occur and are shown in the left hand panel of Figure 5.

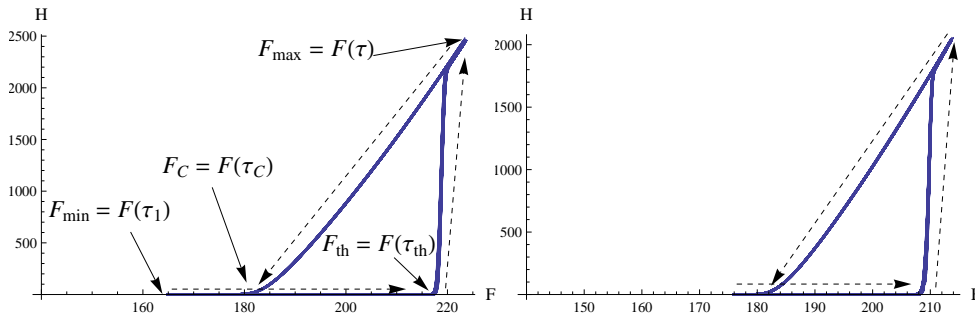


Figure 5. Left: Periodically varying hyperparasite and fluke populations obtained by numerical solution of Eqs. (1) and (2) with $a(t)$ as given by Eq. (4). Parameter values used were as given in Table 1, with $\tau = 5$ in Eq. (4) and $f\lambda/\varepsilon = 5$. Right: Sinusoidally forced system with fluke dynamics given by Eq. (2.7). Here, parameter values used were $a = 10$, $c = 185d$, $d = 1/3000$, $\lambda = 1/300$, $\delta = 1/25$, $\varepsilon = 1/5000$, $f\lambda/\varepsilon = 5$. Quantitative differences between populations under the two immigration scenarios are due to different parameter sets e.g. maximum hyperparasite population is close to 2500 for square wave immigration term and just over 2000 for the sine wave term immigration.

This figure presents the trajectory of a stable T -periodic solution of system (1), (2) and (4). Figure 6 presents the time traces of both of the populations (for clarity, the hyperparasite population is scaled by a constant) over a longer simulation, demonstrating the stability of the system and the presence and absence of the hyperparasite population depending on the oscillation of the fluke population above and below the threshold. In the left hand panel of Figure 5, the fluke population reaches its minimal value F_{min} at the time of the year when the immigration starts, that is at the moment $\tau_1 = 0$ (and then at the same time of the year $t = kT$ every year). At this point, there are no hyperparasites present in the system (more precisely,

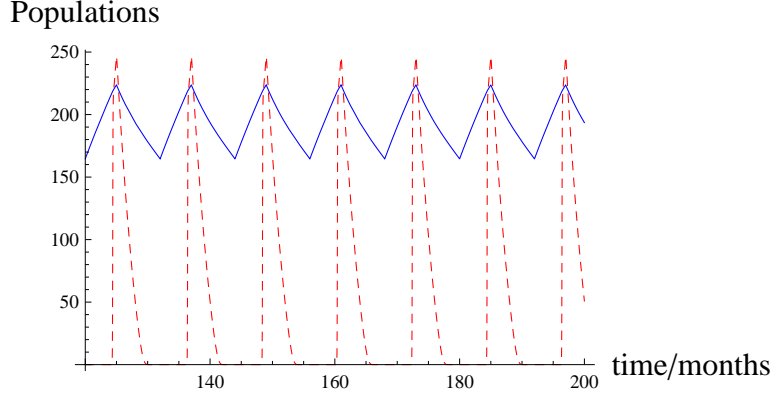


Figure 6. Time trace of the system given by (1), (2) and (4) showing the stable periodic dynamics of the fluke population in blue, hyperparasite population (factor of 1/10) in dashed red, simulated after truncation of the initial variation. Parameters used are as given in Table 1 with $H_0 = F_0 = 100$ at $t = 0$, $\tau = 5$ in Eq. (4) and $f\lambda/\varepsilon = 5$. Yearly periodic behaviour is evident for both populations.

hyperparasites are not detectable as the population H is close to zero and in effect becomes occult). As the fluke population increases with time it eventually reaches a value $F_{th} > F_C$ at a moment τ_{th} , whereby the delayed loss of stability occurs and the system quickly tends to the stable positive branch, $H = \phi_1(F)$ of the critical curve. Further increase in both populations continues, until the instant τ whereupon the fluke population tends to die off through mortality caused by the hyperparasites, together with zero immigration and natural death. The fluke and hyperparasite populations decrease along the positive branch $H = \phi_1(F)$ towards the point $(F, H) = (F_C, 0)$. The hyperparasite population has now collapsed to an exceedingly low level (i.e., becomes undetectable) after the moment τ_C when the fluke population reaches the value F_C . The fluke population continues decreasing to the minimal value F_{min} , which is achieved at the moment T , whereupon the new period begins. As we take monthly time intervals, $T = 12$ in this case.

We see that in the limit of the time separation parameter ε tending to zero, that is, the populations evolve along the critical curve, as indicated in the left panel of Figure 5, the periodic solution is characterised by a few parameters, namely the population values $F_{min} = F(0)$, $F_{th} = F(\tau_{th})$, $F_{max} = F(\tau)$ and the time moments τ_{th} , τ , τ_C . In this limit, the periodic solution follows the zero branch, $H = 0$, between the moments $\tau_1 = 0$ and τ_{th} and the positive parabolic branch, $H = \phi_1(F)$, on the rest of the period, while the transition from the zero branch to the positive branch becomes infinitely fast. It is interesting in this regime to look further at the algebraic consequences due to the ability to integrate the system explicitly.

2.5. Algebraic relations for the limit of the periodic solution

The reduced equation (3) can be integrated explicitly on each branch of the slow manifold. On the time interval $0 \leq t \leq \tau_{th}$, the reduced equation is obtained by setting $H = 0$ and $a(t) = A$, resulting in a linear equation with the solution

$$F(t) = F_A(t) = \frac{A}{\delta} + e^{-\delta t} \left(F_{min} - \frac{A}{\delta} \right). \quad (5)$$

We can immediately deduce the value for one characteristic population,

$$F_{th} = F_A(\tau_{th}) = \frac{A}{\delta} + e^{-\delta\tau_{th}} \left(F_{min} - \frac{A}{\delta} \right).$$

Between the moments τ_{th} and τ_C , when parasites are present after the threshold time and the solution follows the positive branch $H = \phi_1(F)$, the evolution of the fluke population is governed by the reduced equation:

$$\frac{dF}{dt} = \alpha - \delta F - \frac{F}{f}(-c + dF)$$

where $\alpha = A$ on the time interval $\tau_{th} \leq t \leq \tau$ and $\alpha = 0$ on the time interval $\tau \leq t \leq \tau_C$. Separating the variables in this equation and integrating over each of these two time intervals leads to the relations

$$\phi_A(F_{max}) - \phi_A(F_{th}) = \tau - \tau_{th}, \quad \phi_0(c/d) - \phi_0(F_{max}) = \tau_C - \tau,$$

with

$$\phi_\alpha(F) = \int \frac{dF}{\mu F^2 + \nu F + \alpha},$$

where $\mu = -d/f$, $\nu = c/f - \delta$. As the discriminant $\nu^2 - 4\mu\alpha$ of the denominator of the integrand is positive (we neglect the special case where $c/f = \delta$),

$$\phi_A(F) = \frac{1}{\sigma} \log \left| \frac{2\mu F + \nu - \sigma}{2\mu F + \nu + \sigma} \right|, \quad \phi_0(F) = \frac{1}{\nu} \log \left| \frac{2\mu F}{2\mu F + 2\nu} \right|,$$

where $\sigma = \sqrt{\nu^2 - 4\mu A}$.

From the moment $t = \tau_C$ to $t = T$ the solution again follows the zero branch $H = 0$ of the slow manifold, like during the time interval $0 \leq t \leq \tau_{th}$ considered above. However, now $a(t) = 0$ and the reduced equation yields

$$F(t) = F_0(t) = \frac{c}{d} e^{\delta(\tau_C - t)} \quad (6)$$

which gives a result for the minimum fluke population reached, namely,

$$F_{min} = \frac{c}{d} e^{\delta(\tau_C - T)},$$

at the time $t = T$.

Finally, consider the time interval when the parasite population is small, i.e. the trajectory stays near the zero branch of the critical curve from the moment τ_C to the moment $\tau_{th} + T$. The delayed loss of stability phenomenon ensures that, in the limit of vanishing ε , the initial and the final moments of this time interval are related by the integral equation

$$\int_{\tau_C}^{\tau_{th} + T} (-c + F(t)d) dt = 0, \quad (7)$$

see for example Butuzov *et al.* (2004). This relation follows from the explicit solution of the linearised Eq. (2) at $H = 0$,

$$\varepsilon \frac{dH}{dt} = (-c + dF)H;$$

the solution reads

$$H(t) = H(t_0) \left(\text{Exp} \left[\frac{1}{\varepsilon} \int_{t_0}^t (-c + F(t) d) dt \right] \right)$$

with a large parameter $1/\varepsilon$ under the exponent. We see that $H(t) = H(t_0)$ if the integral under the exponent is zero, which leads to the relationship (7) between the moments τ_C and $\tau_{th} + T$ in our model.

Using the periodicity of the solution and substituting the expressions (5), (6) for F on the time intervals $0 \leq t \leq \tau_{th}$, $\tau_C \leq t \leq T$ in Eq. (7), we obtain

$$c\tau_C - cT - \frac{c}{\delta} e^{\delta(\tau_C - T)} + \frac{c}{\delta} - c\tau_{th} + \frac{dA\tau_{th}}{\delta} + \left(\frac{1}{\delta} - \frac{e^{-\delta\tau_{th}}}{\delta} \right) \left(dF_{min} - \frac{dA}{\delta} \right) = 0.$$

In summation, we have obtained five equations with five unknown parameters, namely F_{min} , F_{max} , F_{th} , τ_C , τ_{th} , of the periodic solution, in the limit of small ε :

$$\begin{aligned} F_{th} &= \frac{A}{\delta} + e^{-\delta\tau_{th}} \left(F_{min} - \frac{A}{\delta} \right), \\ \phi_A(F_{max}) - \phi_A(F_{th}) &= \tau - \tau_{th}, \\ \phi_0\left(\frac{c}{d}\right) - \phi_0(F_{max}) &= \tau_C - \tau, \\ F_{min} &= \frac{c}{d} e^{\delta(\tau_C - T)}, \\ c\tau_C - cT - \frac{c}{\delta} e^{\delta(\tau_C - T)} + \frac{c}{\delta} - c\tau_{th} + \frac{dA\tau_{th}}{\delta} + \left(\frac{1}{\delta} - \frac{e^{-\delta\tau_{th}}}{\delta} \right) \left(dF_{min} - \frac{dA}{\delta} \right) &= 0. \end{aligned} \tag{8}$$

2.6. Numerical results

The set of Eqs. (8), can be rewritten to yield two equations with two unknowns, $\psi_1(\tau_{th}, \tau_C) = 0$ and $\psi_2(\tau_{th}, \tau_C) = 0$. These equations are not given explicitly here as their form does not contribute any additional information to understanding of the problem.

Using the known set of parameter values given in Table 1, a plot of both functions gives an estimate for a point of intersection. This estimate is then used to numerically calculate the point of intersection giving the actual values of τ_{th} and τ_C . For the parameter set used in Table 1 and $\tau = 5$ in Eq. (4), the graphical output is shown in Figure 7. The actual solution found using the estimates from the plot yields $\tau_{th} = 4.3$ months and $\tau_C = 9.1$ months.

Using the results for τ_{th} and τ_C , we obtain other parameters from the relational equations. That is, we find that

$$F_{th} = 218, F_{min} = 165, \text{ and } F_{max} = 223.$$

Using the algebraic relations to calculate results as above, it is interesting to compare the numerical solutions with the theoretical infinitely fast transition between both branches in the limit $\varepsilon \rightarrow 0$. Figure 8 indicates this with the threshold point $F_{th} = 218$ calculated from above. A close correlation between numerics and the limit solution obtained from Eqs. (8) is evident.

2.7. Sinusoidal immigration term

To confirm the applicability of the model, another variation to the immigration of flukes into the cockle is considered, namely that of using a sinusoidal type immigration, as mentioned already. We state this new modification by changing the immigration term in Eq. (1) to

$$\frac{dF}{dt} = a(1 + \sin(2\pi t/T)) - \delta F - \lambda H,$$

where the immigration rate is periodic with the period T of one year. Immigration begins again at time $\tau_1 = 0$ where the fluke population is at its minimum F_{min} . The dynamics follow the same pattern as described above, shown in the right hand panel of Figure 5 demonstrating that the qualitative dynamics of the model remain unchanged. However, this type of model does not give us explicit algebraic relations for parameters of the periodic solution in the limit $\varepsilon \rightarrow 0$.

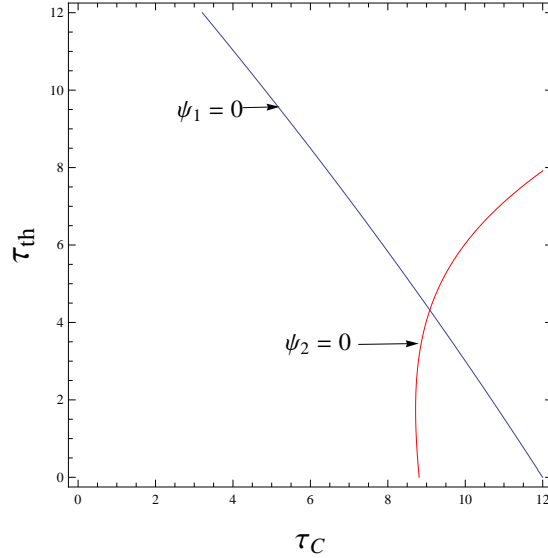


Figure 7. Plot showing intersection of the functions $\psi_1 = 0$ and $\psi_2 = 0$ for estimating τ_{th} and τ_C . Parameters are as given in Table 1, with $\tau = 5$ in Eq. (4) and $f\lambda/\varepsilon = 5$.

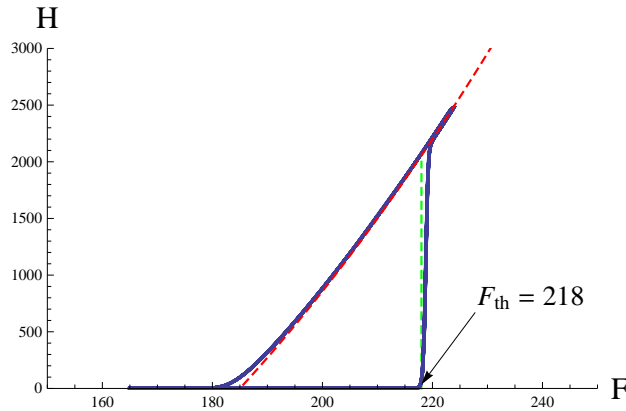


Figure 8. Numerical simulation of the parasite population as a function of fluke population (solid) showing the critical curve and infinitely fast transition (dashed) at the point $F_{th} = 218$ obtained in the limit $\varepsilon \rightarrow 0$ from algebraic Eqs. (8) for the parameter set in Table 1.

3. Bird-Shellfish-Parasite model

In the previous section, we have considered a model demonstrating the threshold effect observed for the hyperparasite population to grow and persist in a single cockle, depending on the number of flukes present. We now extend the model to include other species that have an impact on flukes-hyperparasite subsystem, see Figure 1. This can help understanding of the importance that the hyperparasite plays, not just to cockle health, but to the entire ecosystem in bay areas. The periodic immigration terms we used in the flukes equation are artificial, as the actual immigration is derived from the seasonal migration of birds to and from the area. Therefore, we attempt to model the threshold phenomenon using more realistic dynamics related to both the carriers of the initial infection, that is the birds, and the platform for mass reproduction, that is the mollusc *S. plana*. The aim of this section will be to describe each population individually

but yet maintain the threshold of an average number of 185 flukes per cockle necessary for the hyperparasite population to grow and persist.

3.1. Oystercatcher population

It can be seen from Figure 1 that the driving force behind the dynamics of the fluke life-cycle is the Oystercatcher (*Haematopus ostralegus*) population. These are the definitive host of the fluke and are the link between the fluke in cockle and those entering *S. plana*, so as to provide a new cycle of immigration and infection. That is, they play the necessary part of closing the life-cycle of the fluke. We refer to these Oystercatchers simply as birds. These birds are also the main predators of the cockle population. Therefore, it is beneficial for the fluke to have birds eat as many cockles as possible, to result in high levels of infection. A break in this point of the chain would mean no flukes present and in turn, no hyperparasites, once the lower limit of the threshold is reached. The fact that the birds consume huge numbers of cockles is itself of interest to the system. Questions as to the lower numbers of cockles needed to entice birds to an area can be asked.

Since these birds are migratory, we introduce a periodic forcing term. We allow the bird population B to follow a basic logistic equation, modified however to be dependent on the cockle population C . This ensures that low numbers of cockles lead to birds having less interest in returning to, or coming to, the area. It is, however, evident that they have an ability to prey on food sources other than that of cockles, but the cockle does provide the main source of food for these birds and thus provides the major stimulus for bringing birds to the area. Thus, the equation for the bird population B will be given by

$$\frac{dB}{dt} = kp(t)CB + k_0B - sB^2,$$

where the migration $p(t)$ is periodic with 12 month cycles; k is a scaling coefficient. It is observed that birds migrate to area's of Ireland in large numbers for Winter months, with peak numbers seen between September and March (Birdwatch Ireland. <http://www.birdwatchireland.ie/Default.aspx?tabid=314>; accessed 8th March 2012). This forcing term is adjusted to allow for these dates to influence the migratory patterns. As an approximation, we set up the forcing function $p(t)$ so as bird immigration begins on the 10th month, that is October, and all birds leave at the beginning of January; in the interim, there is an added period of growth in bird population, see the left panel of Figure 9.

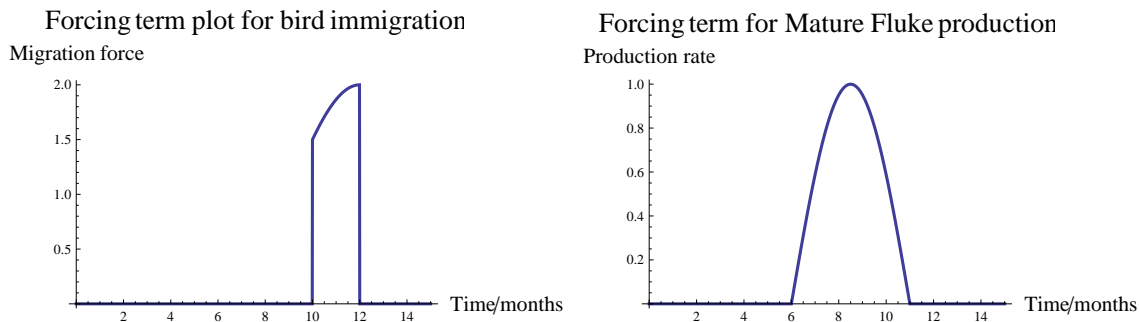


Figure 9. Left: The bird migration forcing term $p(t)$ showing immigration beginning in October, continuing at a declining rate until the end of December, and birds leaving the area in January. This is periodic on a 12 month interval. Right: Plot showing the forcing function $\kappa(t)$ for mature fluke production. Mature flukes were found to be actively swimming and capable of infecting cockles from June (month 6) to November (month 11).

The growth in logistic form due to cockles is accounted for by the CB of the first term and the competition between birds, by the last term. The second term allows for a growth in the bird population even with low cockle numbers indicating alternative food sources. It should be noted that we assume all birds are carriers of the fluke, or at least pick up the fluke infection immediately on returning to an area with infected cockles, and so all of the population can spread flukes to *S. plana*. This assumption is supported by the fact that most areas with fluke infections show cockles with a prevalence of over 80% and reaching 100% (Fermer *et al.*, 2010) and the observation that the birds are each capable of eating in excess of 500 cockles per day.

3.2. Scrobicularia plana populations

We refer to *S. plana* just as plana, and we make an initial assumption here that it is reasonable to divide the population into an overall constant population P_0 , and the subgroup of fluke-infected plana, $P_I = P_I(t)$. The infected plana population grows due to susceptible plana $P_0 - P_I(t)$ encountering flukes in an infectable stage, that is, those deposited by birds. The population decreases due to a recovery term whereby infected plana recover to carry no flukes. Thus we assume growth in the infected population proportional to the product of the susceptible plana and bird populations, and decline proportional to infected plana, that is standard infection-recovery terms:

$$\frac{dP_I}{dt} = \xi B(P_0 - P_I) - \gamma P_I.$$

According to Fermer *et al.* (2010), the prevalence of fluke infection in plana ranged from over 10% to nearly 25% over the course of a year. The numbers of plana in an area was also found to be much less than those of cockles. Due to the possible high densities of cockles, we assume cockle populations in an area to be of the order of millions. It seems a reasonable assumption that an overall plana population of tens of thousands in an area is acceptable. We use the value of $P_0 = 20000$ and obtain the population of infected plana varying from about 2000 to 5000.

3.3. Fluke populations

The mechanism of flukes progressing through the system is complex and needs to be compartmentalised so as to allow study of individual sections and effects. The model we have chosen is to have a first stage of plana infection, what we call larval flukes, F_{PL} . These are those flukes that initially infect plana from birds. The population will be proportional to the infected plana population ($F_{PL} = \beta P_I$), and we assume small numbers on average per plana. These larval flukes undergo asexual reproduction within the fluke to produce large numbers of mature flukes, F_{PM} , still inhabiting plana. These mature flukes develop only at certain times of the year, so we introduce a periodic forcing term to this equation. The mature flukes go on to infect cockles through emigration from plana and meeting a cockle, but will undergo a death rate either within the plana or during the transmission process, hence we add a natural death rate term to this equation leaving

$$\frac{dF_{PM}}{dt} = r\kappa(t)F_{PL} - \epsilon F_{PM},$$

where the plot of $\kappa(t)$ is shown in right panel of Figure 9; r is a scaling coefficient. These completely developed and freely swimming flukes were observed between June and November, and were the dominant stage from July to October (Fermer *et al.*, 2010).

The next fluke population, F_{CO} , is that proportion of mature flukes that successfully infect a cockle. The number of flukes in cockles should not exceed the number of mature flukes as they have no means of reproducing once inside cockles. The population F_{CO} of flukes in cockles grows proportionally to the product of the mature fluke population and the cockle population, as per

typical infection rate term. They have a natural death rate within the cockle and, importantly, suffer due to parasitism by the hyperparasite. Furthermore, we include an additional term in the equation for F_{CO} . As flukes damage cockles, it is reasonable to assume that they in turn suffer loss as this damage increases. We assume that flukes damage cockles as a parasite giving a term of the form $-\omega F_{CO}$ in the cockle equation, yet to be derived. Therefore, flukes themselves will be lost with a compensating term proportional to $-\omega F_{CO} \times (F_{CO}/C)$. We give the full equation as

$$\frac{dF_{CO}}{dt} = f C F_{PM} - \delta F_{CO} - \nu H - \frac{\zeta \omega F_{CO}^2}{C},$$

where the parameter ζ represents the possibility for over-dispersion as in Eq. (2). Comparing this equation to Eq. (1), the artificial immigration term $a(t)$ is replaced by a dependence on both the cockle population, $C(t)$, and the mature fluke population, $F_{PM}(t)$. The cockle population varies throughout the year due to recruitment and reproduction, as well as predation by birds during Winter months. The second and third terms of both equations remain equivalent. The reason for the additional final term compared to Eq. (1) is because system (1), (2) did not include a measure of cockle damage due to flukes as their population was not relevant to the model.

3.4. Cockle population

The cockle population is assumed to grow logistically in the absence of outside negative effects. It declines due to predation by birds (proportional to the product of cockle and bird populations) and due to fluke damage (proportional to the population of flukes in cockles). The equation is

$$\frac{dC}{dt} = \lambda C - \mu C^2 - \omega F_{CO} - hCB.$$

Parameters ω and h represent the negative parasitic effect of flukes and the predatory effect of birds, respectively.

3.5. Hyperparasite population

The final species we need to model is the hyperparasite. This retains a threshold type behaviour whereby when the population of flukes drops below 185 on average per cockle, the hyperparasite is undetectable. The hyperparasite has a natural death rate, and also a compensating term due its impact on the fluke population, similar to that described earlier for the fluke population and its effect on cockles. The growth rate in this case is reasoned as follows. The hyperparasite population grows following successful transmission to flukes. This occurs within the cockle and so the probability of successful transmission (we can assume that the initial hyperparasite infection remains in a dormant condition prior to infection) will be proportional to an average number of flukes per cockle. Therefore, the probability of successful transmission and growth is proportional to HF_{CO}/C . Again, we assume that hyperparasite population dynamics occur on timescales much less than the other populations, modelled by a small parameter $\varepsilon \ll 1$:

$$\varepsilon \frac{dH}{dt} = -cH + \frac{dHF_{CO}}{C} - \frac{g\nu H^2}{F_{CO}}.$$

Here $c/d = 185$; and g is a coefficient describing over-dispersion. This equation has the same form as Eq. (2), apart from the fact that we now average the recruitment term over the cockle population. This should be reasonable given the amount of homogeneity in a given area.

3.6. Overall system

The system of equations can be summarised as follows:

$$\begin{aligned}
 F_{PL} &= \beta P_I, \\
 \frac{dB}{dt} &= k \left(1 + p \cos\left(\frac{2\pi t}{12}\right) \right) CB + k_0 B - sB^2, \\
 \frac{dP_I}{dt} &= \xi B (P_0 - P_I) - \gamma P_I, \\
 \frac{dF_{PM}}{dt} &= \kappa(t) F_{PL} - \epsilon F_{PM}, \\
 \frac{dC}{dt} &= \lambda C - \mu C^2 - \omega F_{CO} - hCB, \\
 \frac{dF_{CO}}{dt} &= f C F_{PM} - \delta F_{CO} - \nu H - \frac{\zeta \omega F_{CO}^2}{C}, \\
 \epsilon \frac{dH}{dt} &= -cH + \frac{dH F_{CO}}{C} - \frac{g \nu H^2}{F_{CO}}.
 \end{aligned} \tag{9}$$

It is not easy to provide an estimate for the parameters due to their sheer number and the complexity of the system. However, we wish to be left with reasonable population numbers. We have given hints at some of these numbers above; we will now give a more complete description.

A typical density of cockles can be anything around 1000 per square meter. However, it was found that numbers more typical in the south of Ireland were around 100 - 500 (Ferner *et al.*, 2010). Since the typical area of a bay could be of the magnitude of several acres, it is reasonable to assume that a typical cockle population would be of the order of millions. We will use numbers of around three million cockles in total. *S. plana* numbers are much smaller than those of cockles and we use a fixed population of $P_0 = 20,000$ in the area under consideration. The number of those plana actually infected with flukes ranges from about 10% to 25% giving numbers of at least 2,000 to 4,000 infected plana.

Each cockle can be infected with anything from 100 to 3,000 flukes or more (Ferner *et al.*, 2011), meaning the number of flukes in cockles can range from about 10^8 to 10^{10} . These numbers mean that the total number of hyperparasites could be up to the order of 10^{12} or more. The final population, birds, could be assumed at peak times to range in the hundreds to possibly thousands, with essentially absence during warmer Summer months.

3.7. Numerical results

Table 2 presents a typical set of parameters resulting in population numbers within expected ranges for multi-species system (9). In particular, the infected *S. plana* population varies from about 2,000 to over 2,300 during a one year cycle. The cockle population has a low of about 2.8 million and a high of about 3.4 million. The average numbers of flukes per cockle is around 200 with some annual variation, and the corresponding hyperparasite population, always present due to the fluke population remaining above the threshold, around 29,000 per cockle. The bird population dies out, or at least is very small during summer months, and peaks at about 900 during the Winter. The corresponding negative effect that the birds have on cockles can be seen in the dramatic decline in cockle numbers at this time of year. The populations of mature flukes in plana and total numbers of flukes in cockles are also in line with expectations.

3.8. Threshold effect

Figure 10 shows a possibility of the translation of the threshold phenomenon from Eqs. (1), (2) to the more complex system (9). The hyperparasite population is not present for part of the year when the fluke population is lower than the threshold value 185. Once this is reached (or at least, once the exchange of stability occurs) the hyperparasite population grows rapidly, leading to a momentary decline in flukes, before an increase in both populations. There are probably effects of feedback to the system at play here also. The fluke population grows through immigration which is dependent on birds which themselves are dependent on cockles. After this point, there is a steady decline until the fluke population decreases below the threshold and the hyperparasite

population goes to zero until the new season of fluke immigration begins. The parameters used are given in Table 3.

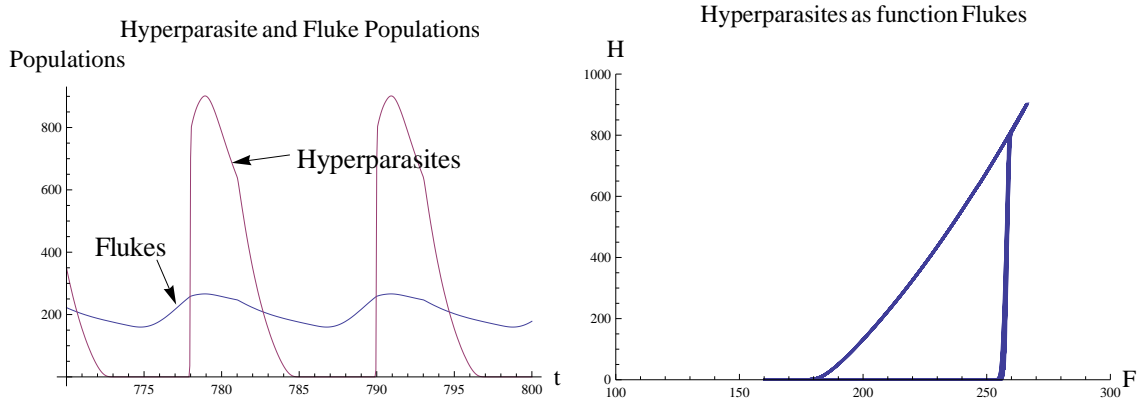


Figure 10. Threshold effect evident for system (9) with parameter values as given in Table 3. Left: Time traces of the fluke and hyperparasite populations. Right: Projection of the periodic solution on the fluke-hyperparasite plane. The hyperparasite can be seen to be absent from the system during periods in which the average number of flukes per cockle drops below 185, that is the threshold type dynamics similar to that demonstrated by system (1), (2), cf. Figure 5.

3.9. The role of the hyperparasite *U. legeri* in the ecosystem

The structure of the interactions of species in Figure 1, and simulations of system (9), suggest that the hyperparasite may play a very important role in the ecosystem. That is, it impacts on the entire system in a much greater way than its relative size would suggest. In order to provide some verification of this hypothesis, we test a scenario where the hyperparasite is effectively removed entirely from the system at some moment in time, and examine the impact that this has on the other populations. The method employed is, using the parameter values as given in Table 2, to solve system (9) for the time $t = 600$ months to ensure that the system reaches the stable periodic regime. From the time $t = 600$ up to the time $t = 1400$, the value of the parameter c is greatly increased. The actual value was increased from $185 d$ to $30,000 d$. This ensures that the hyperparasite is present only in extremely small numbers and is essentially wiped out from the system after the moment $t = 600$. Figure 11 shows the effect that this change has on the cockle population. It can be seen that the change is quite dramatic. With the parasite present, the cockle population varies around 3 million, depending on time of year. In the absence of the hyperparasite, this figure drops to some 700,000 cockles, a drop of over 70%. The effects on birds, infected plana and other populations (not shown) are similar. In fact, the bird and infected plana populations drop by almost 80% after the hyperparasite extinction.

The model (9) does not allow for the populations to become zero. Future work may look at a model where it is possible to better quantify the role of the hyperparasite via a bifurcation scenario.

4. Conclusions

We have developed a preliminary model that describes the observed threshold phenomenon in the cockle system. The interaction of this fluke-hyperparasite system appears to be of considerable interest. Gam *et al.* (2008) in a study of a coastal lagoon in Morocco found a higher prevalence of this fluke in older cockles in the inner lagoon compared to the outer lagoon. One suggestion for the difference in prevalence was the higher rate of hyperparasitism in the outer lagoon, with

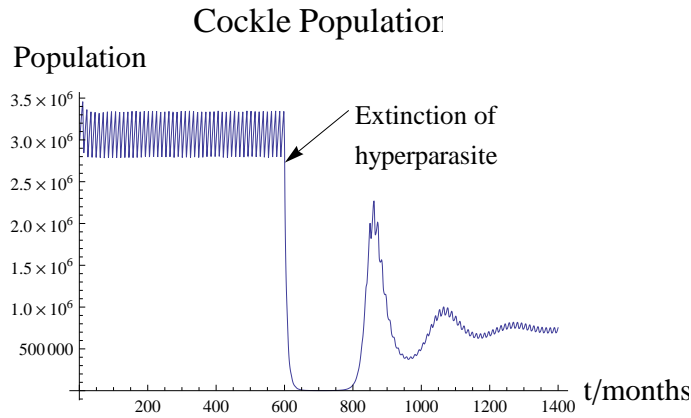


Figure 11. Cockle population in system (9) with parameter values from Table 3. After 600 months, the hyperparasite's death rate is changed to a greatly increased level leading to their extinction. The effect this has on cockles is shown here. A stable periodic solution of over 3 million cockles is reached before the hyperparasite is artificially removed from the system whence there is a dramatic temporary extinction or absence of cockles from the area for almost 200 months. The effects that this could have on an ecosystem may be permanently damaging. However, as the model does not allow for the cockle population to remain completely extinct, after a period of renewal, the cockle population settles to a new periodic pattern varying around the value of 700,000 cockles. Similar effects are seen in the other populations indicating the importance that the hyperparasite has on the system despite its minute size. This effect is indicative that the hyperparasite is a keystone species.

90% of the trematodes being hyperparasited. It was suggested that this hyperparasite infects and kills *M. minutus* and therefore may control infrapopulations of this trematode (James *et al.* 1977).

Through the use of a relatively standard host-parasite model based on those developed over the past number of decades, we introduced the assumption that the hyperparasite dynamics occur in the system on timescales much faster than that of the fluke. Again this is a classical slow-fast system which arises in engineering, biology and physics. The introduction of the small parameter in the parasite equation gives rise to the threshold, below which no parasites are observed. In fact, due to the delayed loss of stability, two thresholds are actually apparent. With the introduction of a mathematical threshold, we examined the scenario whereby switching of the fluke immigration on and off occurs. This was described to be a realistic occurrence due to the periodic nature of fluke maturation in *S. plana*. It should be noted that it has been observed that although fluke populations can develop in young cockles, parasites do not appear until the cockle is over one year old and there also appears to be the building up of a type of immunity towards flukes in later life. Thus there are varying factors in the immigration rate that may need consideration in a future work. We examined immigration effects and, through a simplification of a switch over a sinusoidal type immigration, we showed that it was possible to derive algebraic relations, which accurately define the periodic solution in the limit where the ratio of the fluke and hyperparasite time scales tends to zero. In particular, we observe both delayed and immediate stability exchange in the hyperparasite population and well-defined indicator times and populations that characterise the periodic dynamics and the thresholds. Assuming parameter values, we used the equations relating the unknowns to derive explicitly the moment of the year when hyperparasite populations start to grow. From this it was possible also to find other points such as the maximum and minimum fluke populations, the

threshold fluke population and corresponding times.

Finally, we have considered a seasonally driven multi-species model of an ecosystem shown in Figure 1, which involves bird, and shellfish species typical of a bay or estuarine area, and accounts for typical stages of the parasites' life cycles. We have demonstrated that the persistence threshold effect can be transferred from the cockle-hyperparasite subsystem to the entire ecosystem in this model. We have also provided evidence that the hyperparasite, despite its minute size, can be an important regulator of abundance of co-dependent species in the ecosystem.

Acknowledgments

This work was supported by the European Regional Development Fund (ERDF) through the Ireland Wales Programme (INTERREG 4A). DR acknowledges the support of the Russian Foundation for basic Research through grant 10-01-93112.

References

- [1] R M Anderson and R M May 1978 Regulation and stability of host-parasite population interactions: I. Regulatory processes *Journal of Animal Ecology* **47** 219-247
- [2] J J Beukema and R Dekker 2005 Decline of recruitment success in cockles and other bivalves in the Wadden Sea: possible role of climate change, predation on postlarvae and fisheries *Mar Ecol Prog Ser* **287** 149-167
- [3] E A Bowers *et al.* 1996 The metacercariae of sibling species of *Meiogymnophallus*, including *M. rebecqui* comb. nov. (Digenea: Gymnophallidae), and their effects on closely related *Cerastoderma* host species (Mollusca: Bivalvia) *Parasitology Research* **82** 6 505-510
- [4] V F Butuzov *et al.* 2004 Singularly perturbed problems in case of exchange of stabilities *Journal of Mathematical Sciences* **121** 1973-2079
- [5] X de Montaudouin, I Kisielowski, G Bachelet and C Desclaux 2000 A census of macroparasites in an intertidal bivalve community, Arcachon Bay, France *Oceanologica Acta* **23** 453-468
- [6] X de Montaudouin *et al.* 2009 Digenean trematode species in the cockle *Cerastoderma edule*: identification key and distribution along the north-eastern Atlantic shoreline *Journal of the Marine Biological Association of the United Kingdom* **89** 543-556
- [7] A Deredec and F Curchamp 2003 Extinction thresholds in host-parasite dynamics *Ann Zool Fennici* **40** 115-130
- [8] E S Didier, M E Stovall, L C Green, P J Brindley, K Sestak and P J Didier 2004 Epidemiology of microsporidiosis: sources and modes of transmission *Veterinary Parasitology* **126** 145-166
- [9] J P Ducrotoy *et al.* 1991 A comparison of the population dynamics of the cockle (*Cerastoderma edule*, L.) in North-Western Europe *Estuaries and Coasts: Spatial and Temporal Intercomparisons* M Elliott and J-P Ducrotoy (eds) (Olsen & Olsen) 173-184
- [10] G W Esch, M A Barger and K J Fellis 2002 The transmission of digenetic trematodes: style, elegance, complexity *Integr Comp Biol* **42** 304312
- [11] M Etchechoury and C Muravchik 2003 Nonstandard singular perturbation systems and higher index differential-algebraic systems *Applied Mathematics and Computation* **134** 323-344
- [12] J Fermer 2009 Parasitological investigation of softsediment bivalve, with particular reference to the digenean trematode *Meiogymnophallus minutus* Ph D Dissertation, University College Cork, Ireland, October 2009, 143 pages
- [13] J Fermer *et al.* 2010 Temporal variation of *Meiogymnophallus minutus* infections in the first and second intermediate host *Journal of Helminthology* **84** 362368
- [14] J Fermer *et al.* 2011 Manipulation of *Cerastoderma edule* burrowing ability by *Meiogymnophallus minutus* metacercariae *Journal of the Marine Biological Association of the United Kingdom* **91** 907911
- [15] M Gam, H Bazairi, K T Jensen and X de Montaudouin 2008 Metazoan parasites in an intermediate host population near its southern border: the common cockle (*Cerastoderma edule*) and its trematodes in a Moroccan coastal lagoon (Merja Zerga) *Journal of the Marine Biological Association of the United Kingdom* **88** 357364
- [16] M Gam, X de Montaudouin and H Bazairi 2010 Population dynamics and secondary production of the cockle *Cerastoderma edule*: A comparison between Merja Zerga (Moroccan Atlantic coast) and Arcachon Bay (French Atlantic coast) *Journal of Sea Research* **63** 191-201
- [17] W M Getz and J Pickering 1983 Epidemic models: thresholds and population regulation *Am Nat* **121** 6 892-898

- [18] R F Hechinger *et al.* 2007 Can parasites be indicators of free-living diversity? Relationships between species richness and the abundance of larval trematodes and of local benthos and fishes *Oecologia* **151** 82-92
- [19] J A P Heesterbeek and M G Roberts 1995 Mathematical models for microparasites of wildlife *Ecology of Infectious Diseases in Natural Populations* B T Grenfell and A P Dobson (eds) (Cambridge: Cambridge University Press) 91-122
- [20] R D Holt *et al.* 2003 Impacts of environmental variability in open populations and communities: inflation in sink environments *Theoretical population biology* **64** 315-330
- [21] P J Hudson *et al.* 2006 Is a healthy ecosystem one that is rich in parasites? *Trends in Ecology and Evolution* **21** 7 381-385
- [22] B L James, A Sannia and E A Bowers 1977 Parasites of birds and shellfish *Problems of a Small Estuary* A Nelson-Smith and E M Bridges (eds) (Swansea: Proc Burry Inlet Symposium **1**) 1-16
- [23] P T J Johnson, A Dobson, K D Lafferty, D Marcogliese, J Memmott, S Orlofske, R Poulin and D W Thieltges 2010 When parasites become prey: ecological and epidemiological significance *Trends in Ecology & Evolution* **25** 362-371
- [24] L Kalachev, T C Kelly, M J O'Callaghan, A V Pokrovskii and A A Pokrovskiy 2010 Analysis of threshold-type behaviour in mathematical models of the intrusion of a novel macroparasite in a host colony *Math Med Biol* **28** 4 287-333
- [25] A M Kuris *et al.* 2008 Ecosystem energetic implications of parasite and free-living biomass in three estuaries *Nature* **454** 515-518
- [26] G Lauckner *et al.* 1983 Diseases of mollusca: Bivalvia *Diseases of Marine Animals Vol. 2 Introduction, Bivalvia to Scaphopoda* O Kinne (ed) (Hamburg: Biologische Anstalt Helgoland) 477-961
- [27] K N Mouritsen and R Poulin 2002 Parasitism, community structure and biodiversity in intertidal ecosystems *Parasitology* **124** S101-S117
- [28] M Nizette, D Rachinskii, A Vladimirov and M Wolfrum 2006 Pulse interaction via gain and loss dynamics in passive mode locking *Physica D: Nonlinear Phenomena* **218** 1 95-104
- [29] T R Raffel *et al.* 2008 Parasites as predators: unifying natural enemy ecology *Trends in Ecology and Evolution* **23** 11 610-618
- [30] K Rohde 1994 Niche restriction in parasites: proximate and ultimate causes *Parasitology* **109** S69-S84
- [31] F Russell-Pinto 1990 Differences in infestation intensity and prevalence of hinge and mantle margin *Meiogymnophallus minutus* Metacercariae (Gymnophallidae) in *Cerastoderma edule* (Bivalvia): Possible species coexistence in Ria de Aveiro *J Parasitology* **76** 5 653-659
- [32] F Russell-Pinto *et al.* 2006 Digenean Larvae parasitizing *Cerastoderma Edule* (Bivalvia) and *Nassarius Reticulatus* (Gastropoda) from Ria de Aveiro, Portugal *J Parasitology* **92** 2 319-332
- [33] D W Thieltges and K Reise 2006 Metazoan parasites in intertidal cockles *Cerastoderma edule* from the northern Wadden Sea *Journal of Sea Research* **56** 284-293
- [34] E R Troemel *et al.* 2008 Microsporidia Are Natural Intracellular Parasites of the Nematode *Caenorhabditis elegans* *PLoS Biol* **6** 12 e309
- [35] V Veliov 1997 A generalization of the Tikhonov Theorem for singularly perturbed differential inclusions *Journal of dynamical and control systems* **3** 291-319
- [36] A M Wegeberg and K T Jensen 1999 Reduced survivorship of *Himasthla* (Trematoda, Digenea)-infected cockles (*Cerastoderma edule*) exposed to oxygen depletion *Journal of Sea Research* **42** 4 325-331
- [37] A M Wegeberg and K T Jensen 2003 In situ growth of juvenile cockles, *Cerastoderma edule*, experimentally infected with larval trematodes (*Himasthla interrupta*) *Journal of Sea Research* **50** 1 37-43

Parameter	Value
β	10
k	8×10^{-6}
p	$0 \leq p(t) \leq 2$
k_0	0.088
s	0.054
ξ	8×10^{-6}
P_0	20,000
γ	0.014
r	50,000
κ	$0 \leq \kappa(t) \leq 1$
ϵ	0.06
λ	0.15812
μ	2×10^{-8}
ω	0.0004
h	0.0001
f	3.33×10^{-7}
δ	0.1
ν	0.05
ζ	8
ε	0.001
c	$185d$
d	0.0667
g	0.03

Table 2. Parameters used for numerical simulations of system (9).

Parameter	Value
β	10
k	10^{-6}
p	$0 \leq p(t) \leq 2$
k_0	0.88
s	0.054
ξ	10^{-5}
P_0	20,000
γ	0.01
r	25,000
κ	$0 \leq \kappa(t) \leq 1$
ϵ	1
λ	0.15
μ	2×10^{-8}
ω	0.00025
h	0.00009
f	1.25×10^{-7}
δ	0.0001
ν	0.0256
ζ	0.00025
ε	0.0001
c	$185d$
d	0.0014
g	1.3

Table 3. Parameters used for numerical simulations of system (9).